SIGNAL PROCESSING FOR PULSED ULTRASONO-OPTICAL TOMOGRAPHY

K. Nakayama, Y.Kunihiro and M.Fujii

Department of Electrical and Electronics Engineering, Sophia University, Tokyo, Japan
nakym@kiyoshi.ee.sophia.ac.jp

Abstract: We study NIR tomographic imaging based on the pulsed-ultrasound modulation of diffuse light in turbid media. The main difficulty of the method is the very low S/N which cannot be overcome by the conventional signal-averaging because of the slowly-varying light phase on the detector. We proposed a simple model for the detected signal and validated it experimentally. Furthermore, we proposed frequency -doubling-and-veraging method to recover the signal, and demonstrated its feasibility through the phantom experiment.

Introduction

Although the diffuse NIR medical imaging has become an increasingly active research field, its clinical applicability is still limited mainly because of the poor spatial resolution due to the highly scattering nature of the tissue. As one possibility to overcome this defect, the ultrasound modulation of the diffuse light has been investigated by several researchers [1]-[3] The diffuse light in turbid media is modulated by the ultrasound due to Doppler effect and this modulated light should reflect the local optical property. Thus the ultrasono-optical system may potentially image the NIR properties of the living bodies with the spatial resolution of the diagnostic ultrasound. We have been investigating the pulsed-ultrasound modulation, which seems promising for the quasi-real-time operation. The difficulty in pulsed ultrasono-optical tomography arises from the extremely small modulation of light by the ultrasound at the modulation site. The signal detectability is further degenerated by the destructive summation of the signal at the detector aperture. Moreover, the signal to noise ratio cannot be improved by conventional time averaging because the signal cannot be assumed stationary. In this report, we propose a simple model for the signal from the photodetector and confirm it experimentally. We also propose a signal processing scheme based on the proposed signal model and assesed the performance by simulation. We demonstrate the feasibility of the pulsed ultrasono-optical tomography experimentally based on the proposed signal processing scheme.

Signal Model

When light having unit amplitude of electric field is incident to a scatterer at position $\mathbf{r}_0$ moving by the ultrasound, the scattered electric field of light at position $\mathbf{r}$ can be expressed as follows;

$$E_{mod}(t) = \exp(j\omega_0 t)\cdot\exp\left[-jk\mathbf{i}\bullet\left\{\mathbf{r}_o+\xi\,\hat{\mathbf{s}}\cos\left(\omega_{u_s}t+k_{u_s}\hat{\mathbf{s}}\bullet\mathbf{r}_0\right)\right\}\right]\cdot\frac{f(\hat{\mathbf{i}},\hat{\mathbf{o}})}{|\mathbf{r}-\mathbf{r}_0|}\exp\left[-jk\hat{\mathbf{o}}\bullet\left\{\mathbf{r}-\left\{\mathbf{r}_o+\xi\,\hat{\mathbf{s}}\cos\left(\omega_{u_s}t+k_{u_s}\hat{\mathbf{s}}\bullet\mathbf{r}_0\right)\right\}\right\}\right]$$
$$= K\exp\left[-jk\left(\hat{\mathbf{i}}-\hat{\mathbf{o}}\right)\bullet\hat{\mathbf{s}}\xi\cos\left(\omega_{u_s}t+k_{u_s}\hat{\mathbf{s}}\bullet\mathbf{r}_0\right)\right] \quad (1)$$

$$K\equiv\exp(j\omega_0 t)\cdot\exp\left[-jk\left\{\left(\mathbf{i}-\hat{\mathbf{o}}\right)\bullet\mathbf{r}_o+\hat{\mathbf{o}}\bullet\mathbf{r}\right\}\right]\cdot\frac{f(\hat{\mathbf{i}},\hat{\mathbf{o}})}{|\mathbf{r}-\mathbf{r}_0|} \quad (2)$$

where ω_o denotes light angular frequency, $k\mathbf{i}$ and $k\mathbf{o}$ denote the incident and scattered light vectors, respectively, and f(i,o) represents the scattering amplitude. Also in eq.(1), ω_{us} denotes ultrasound angular frequency, $k_{us}\mathbf{s}$ denotes the ultrasound wave vector and ξ denotes the amplitude of displacement of the scatterer by ultrasound.

Eq.(1) expresses that light is phase modulated by ultrasound. In actual circumstances, however, the modulation index is extremely small;

$k(\hat{\mathbf{i}}-\hat{\mathbf{o}})\cdot\hat{\mathbf{s}}\xi << 1$,

then,

$$E_{mod}(t) = K\left(1-jk\left(\hat{\mathbf{i}}-\hat{\mathbf{o}}\right)\bullet\hat{\mathbf{s}}\xi\cos\left(\omega_{u_s}t+k_{u_s}\hat{\mathbf{s}}\bullet\mathbf{r}_0\right)\right) \quad (3)$$

Eq.(3) means that scattered light is effectively amplitude modulated by the ultrasound.

We rewrite the modulated part of light in eq.(3) at the detector as follows,

$$E_S(t) = A\cos(\omega_{us}t+\phi_{us})\cos\left(\omega_0 t+\theta_{opt}\right) \quad (4)$$

where ω_o is angular frequency of light, and $\theta_{opt}(t)$ is the phase of the signal light. In eq.(4) also, ω_{us} is ultrasound angular frequency, and $\varphi_{us}(t)$ is the ultrasound phase shift at the scatterer in reference to the transmitted ultrasound signal. This modulated signal light is stationary if we consider the modulated light from one stationary scatterer. But there are many scatters and also the photon experiences multiple scattering so that modulated light at the detector is the summation of many multiply scattered light. Besides, the scatters are subjected to the Brownian motion. Accordingly, the modulated light at the detector becomes random signal, that is, A and θ_{opt} in eq.(4) are random variables which fluctuate slowly in the time domain.

Background non-modulated light at the detector also has random nature since it is the summation of scattered waves from all over the medium. The background light can be expressed as,

$$E_0(t) = B\cos(\omega_0 t+\theta_0) \quad (5)$$

where B and θ_0 are random variables.

Since the photo detector current is proportional to the square of the electric field, and considering A >> B, the detected AC component I_{ac} can be expressed as,

ISSN: 1727-1983

$$I_{ac} \propto 2AB \cos\theta_i(t)\cos(\omega_{us}t + \phi_{us}) \quad (6)$$

The light phase difference $\theta_i(t) = \theta_{opt} - \theta_0$ would fluctuate slowly in the time course because of the Brownian motion of the target scatterers generating the modulated light E_S and/or the background scatterers generating the background unmodulated light E_0 on the detector. Thus the detected AC signal time series of ultrasound frequency would be either in-phase or 180° out-of-phase each other,

$$\begin{aligned} s_i &= c_i(t)\cos\theta_i(t)\cos(\omega_{us}t + \phi_{us}(t)) \\ &= c_i(t)\,|\cos\theta_i(t)|\cos(\omega_{us}t + \phi_{us}(t)) \quad \text{for } \theta_i(t) \geq 0 \\ &\quad c_i(t)\,|\cos\theta_i(t)|\cos(\omega_{us}t + \phi_{us}(t) + \pi) \quad \text{for } \theta_i(t) < 0 \end{aligned} \quad (7).$$

The discussion so far implicitly assumes the detector smaller than the light speckle size. For the realistic detector size, $\theta_i(t)$ would be also spatially random and uniformly distributed between 0 and 2π over the detector surface with the correlation scale of light speckles. Although this causes serious problem of signal reduction at the detector, the nature of the detected signal expressed by eq.(7) would not be changed.

Signal Processing and Simulation

In order to take full advantage of the detected signal nature discussed above, we squared the signal so that the 180° out-of-phase signal in the original ultrasound frequency becomes in-phase in the doubled frequency range. Accordingly, the frequency-doubling-and-averaging would increase the S/N.

We consider coherent pulse echo system, in which the ultrasound pulses are transmitted periodically in phase with the master oscillator of ultrasound frequency f_{us}, conceptually.

Taking time t relative to the i-th pinging of the ultrasound transducer, i-th received optical signal sample can be represented as,

$$x_i(t) = c_i(t)\cos\theta_i(t)\cos(\omega_{us}t + \phi_{us}(t)) + n_i(t) \quad (8)$$

First term in eq.(8) is the signal. If the scatterers position is stationary in the ultrasound wavelength scale, factors in the first term are constant, sample to sample, except for the factor $\cos\theta_i(t)$. Since noise term is typically predominated by the shot noise of the optical detector, the second term in eq.(8) is random independently sample to sample. Therefore, if the ultrasound pulse repetition is very much frequent comparing with the fluctuation of the signal term, simple averaging of the consecutively received samples would be effective to increase S/N. Thus we adopted two stage avraging, firstly conventional averaging, then frequency-doubling-and averaging of the pre-averaged samples.

We assessed the effectiveness of the proposed signal processing by a simulation as follows.

Basic parameters and assumptions are summarized in Table 1, and the results are summarized in Figure.1.

In Figure 1, (a) shows the fluctuation of θ_i which was generated by a random walk process. Abscissa is the sample number. Since the pulse repetition frequency is

Table 1 Simulation parameters

ultrasound frequency 1MHz; pulse repetition frequency 1kHz; For simlicity, it was assumed in eq.(8); $c_i(t) = 0 \quad for \;\; 0 \leq t \leq 51\mu s$ $= 1 \quad for \;\; 52\mu s \leq t \leq 102\mu s;$ $\phi_{us}(t) \equiv 0;$ $\theta_i(t)$: generated by a random walk process. $n_i(t)$: carrier-band normal noise center frequency: 1MHz effective bandwidth: 200kHz.

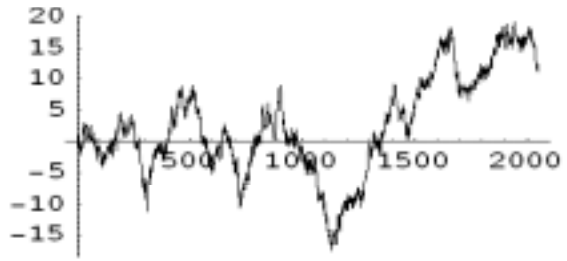

(a) fluctuation of θ_i

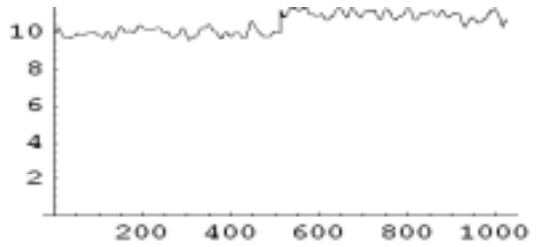

(b) power of the whole sample average

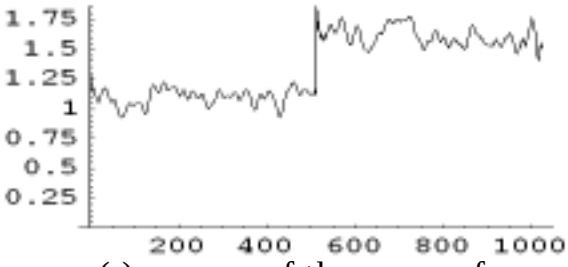

(c) average of the power of preaveraged samples

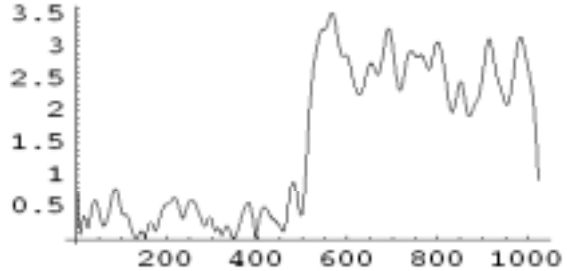

(d) proposed processing

Figure 1: Comparison of various processing

ISSN: 1727-1983

1 kHz, the whole time course is 2.048 sec. Using these θ_i values, we prepared 2048 series of simulated data samples; each data sample is of 102.4μs length of which first 51.2μs is of pure noise and the last 51.2μs is signal plus noise with S/N of -10dB. In Fig. 1, three output data of different averaging scheme are shown. The output (b) is the power of conventional simple averaging of whole samples. Apparent output image S/N calculated from the ratio of the average of last half segment and the average of first half segment is 0.406dB (=10log1.10), which is quite reasonable because signal and noise are independent random process. Since the timecourse of θ_i shown in (a) suggests that original signal is rather slowly varying, we pre-averaged 8 series each and averaged 256 power timecourse of the pre-averaged signals, which results in output (c), of which apparent image S/N is increased to 1.647dB. Finally, output (d) is the result of the proposed processing, which is the magnitude of the frequency-doubled component of the squre of the pre-averaged signals. The apparent image S/N of output (d) is 8.56dB demonstrating the effectiveness of the proposed signal processing.

Experiments

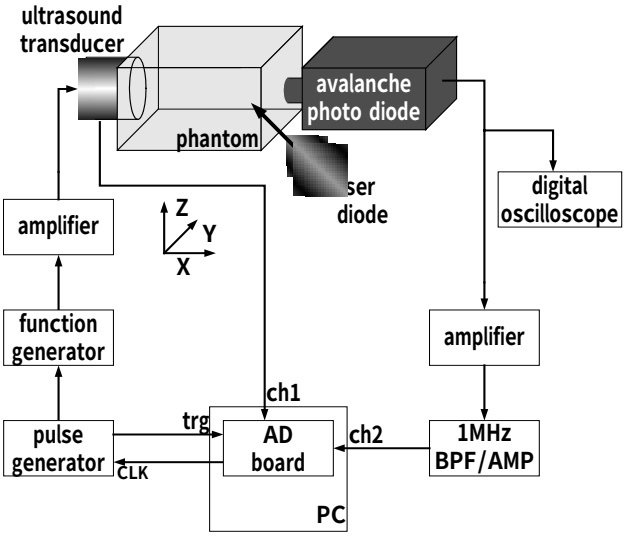

Figure 2: Experimental setup

Fig.2 shows the experimental setup. We performed two experiments using this seup.

Experiment #1 was designed to validate the proposed signal model. A 8X4X3cm phantom was made of agar dispersed with kaolin, of which concentration was adjusted to give the background reduced scattering coefficient of around 0.1mm^{-1}. The high scattering region of 1.5X1.8X3cm was embedded, of which reduced scattering coefficient was adjusted 5mm^{-1}. The phantom was obliquely illuminated by the laser diode (5402, SDL, CA) of 50mW power, wavelength of 780nm and coherent length of several meters. The beam size was about 2mm in diameter on the surface of the phantom. The ultrasound transducer (113-261-360, Krautkramer Branson, PA) of 2.54 cm in diameter, 5cm focal length and 1 MHz center frequency was placed on the other side of the phantom. The 10μs-long 1MHz burst with the repetition frequency of 1kHz from the function generator (FG-161, NF, Japan) was amplified by the power amplifier (150C, KEI, WA) and drove the ultrasound tra nsducer. An avalanche photo diode (APD: C5410, Hamamatsu Photonics, Japan) of 1.5mm aperture was used as the optical detector. The detector output was amplified (8447, Hewlett-Packard), band-pass filtered with the center frequency of 1MHz and the effective bandwidth of 100kHz, and fed to the AD board (PCI-3525, Interface, Japan) which has 10bits resolution with 10MHz sampling rate.

In Experiment #2 which was designed for preliminary 2-D imaging, we drove the transducer with 3μs-long 1MHz burst to obtain better spatial resolution. The phantom was similar but of different size from the one used in the Experiment #1. The laser beam incidence was also different; in experiment #2, transmission type irradiation was adopted whereas irradiation was of reflection type in experiment #1. To obtain 2-D image data, the phantom was mechanically scanned in Z direction.

In both experiments #1 and #2, signals were pre-averaged 100 times, and 1000 pre-averaged signals were analyzed and/or used for the imaging.

Results and Discussion

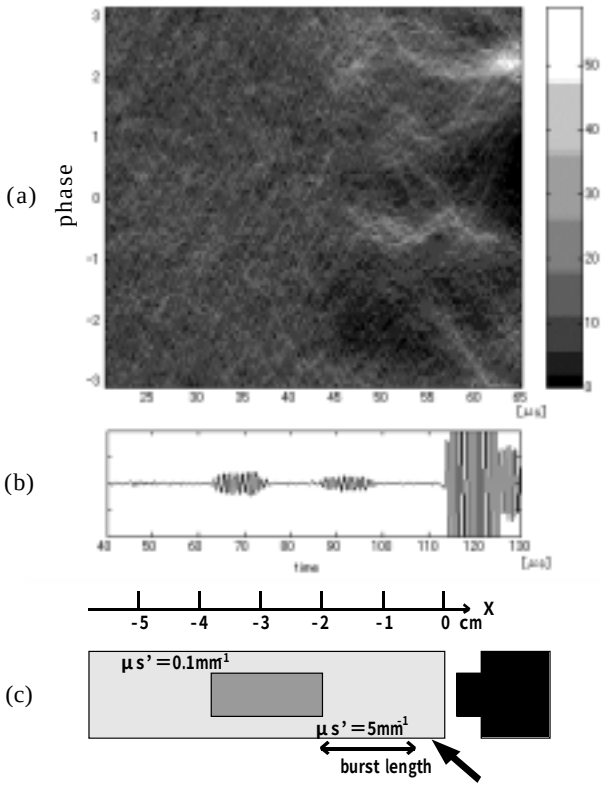

Figure 3: Histogram of the phase timecourse

ISSN: 1727-1983

Figure 3 shows the results of experiment #1. Fig.3(a) is the histogram of the phase timecourse of the 1000 pre-averaged signals. The abscissa of Fig.3(a) is the time from the pinging of the ultrasound pulse, the ordinate is the phase of the signal in radian and the brightness is the histogram. Fig.3(b) indicates the corresponding ultrasound echo. Note that the time scale of (b) is doubled compared with (a) because the ultrasound echo returs twice as late as the time when the ultrasound pulse generates optical echo. Fig.3(c) indicates the correponding phantom geometry. In the region -2<x<0, one can see the phase of the signals are clustered into two groups of which difference is roughly π. This finding strongly supports our signal model.

Fig.4 shows a part of the results of experiment #2 which demonstrates the effectiveness of the proposed signal processing. The upper trace (a) is the result of conventional averaging of 1000 pre-averaged data. We can't recognize any plausible signal corresponding to the phantom geometry. On the other hand, in the trace (b) which is the result of the proposed processing we can recognize the signal. corresponding to the inclusion to the inclusion in the phantom. One may also note large signal at x=-4 and x=0; the former correponds to the beam injection poin and the latter corresponds to the end surface of the phantom.

Finally, Fig. 5 shows the 2D image obtained by scanning the transducer in z-direction. The frequency-doubling-and-averaging method clearly depicted the high scattering inhomogeneity, whereas the conventional averaging failed to image the inclusion.

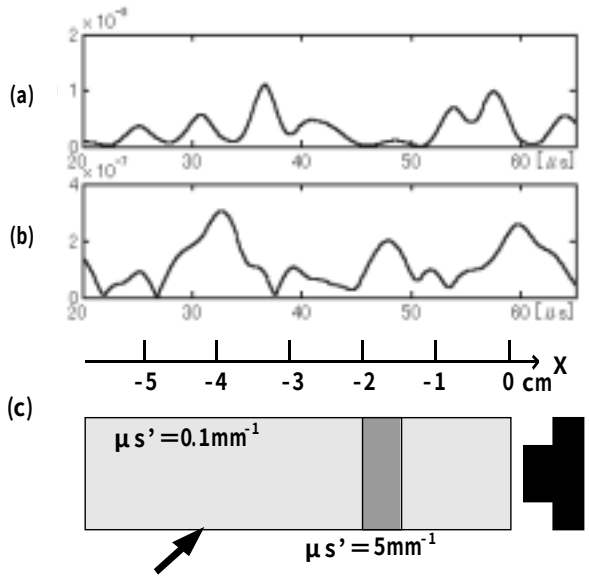

Figure 4: 1-dimensional signal at Z=0
(a) Conventional averaged signal, (b) Averaged frequency-doubled signal, (c) phantom geometry

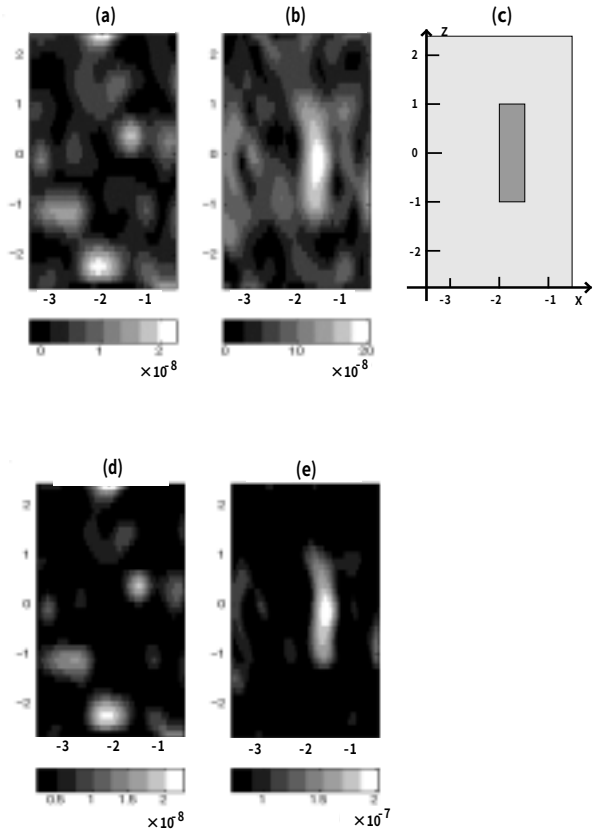

Figure 5: 2-dimensional image
(a) Conventional averaging, (b) Frequency-doubling-and-averaging, (c) phantom geometry, (d) Thresholding image (a) above the shotnoise level estimated from the d.c. component of the detector, (e) Thresholding image(b) above the shotnoise level.

Conclusion

We proposed a simple model for the detected signal and the proposed signal model was confirmed experimentally. Based on the signal model we proposed frequency-doubling-and-averaging method and also confirmed its effectiveness by simulation and through experiment. We successfully demonstrated the feasibility of the pulsed ultrasono-optical tomography on the agar phantom experiment. We believe the method will become the new modality in the field of medical imaging .

References

[1] Wang L-H., Jacques S.L. and Zhao X. (1995): 'Continuous-wave ultrasonic modulation of scattered laser light to image objects in turbid media', *Opt.Lett.*, **24**, pp. 629-631

[2] Kempe M., Laionov D., Zaslevsky D. and Genack A.Z. (1997): 'Acousto-optics tomography with multiply scattered light', *J.Opt.Soc.Am.A.*, **14**, pp. 1151-1158

[3] Lev A. and Sfez B.G. (2003)): 'Pulsed ultrasound-modulated light tomography', *Opt.Lett.*, **28**, pp. 1540-1551

ISSN: 1727-1983